Letters

Method of Early Failure Detection for Elastic Diaphragms Based on Frequency Analysis of the Acoustic Signal

Razvan Ciocan, *Student Member, IEEE*, and Nathan Ida, *Senior Member, IEEE*

***Abstract*—A method of in-service early failure detection based on frequency analysis of the acoustic signal obtained from elastic diaphragms in air-driven pumps is described. A fully digital system for frequency analysis based on a personal computer was developed with a view to practical implementation of this method. The validity of the method was demonstrated by experiments performed under realistic in-plant conditions.**

I. Introduction

An elastic diaphragm is the main part of air-driven pumps that are used in a wide range of applications. The substances carried by this type of pump include: aggressive fluids such as solvents, radioactive waste, and gunpowder. In the event of failure of the diaphragm, leakage of the substance being pumped may occur through the air-exhaust valve. The importance of this occurrence depends on the nature of the fluid being pumped, but in many cases the consequences may be far-reaching.

Monitoring of the diaphragm behavior by inserting displacement devices or sensors inside pumps has had only limited success. The authors propose a method based on the frequency analysis of the acoustic signal emitted by the elastic diaphragm during normal operation. This is a noncontact, nondestructive technique that is external to the diaphragm, and indeed to the pump itself.

II. Principle of the Method

Typically, an air-driven pump will contain two diaphragms driven by a common piston. The diaphragms act as separation membranes between the compressed air supply (10 in Fig. 1) and the liquid to be pumped (13 in Fig. 1). The diaphragm is clamped on its circumference. From a mathematical point of view, the diaphragm can be viewed as a thin circular plate and the exact solution for the differential equation that describes its oscillation is given in [1]. The Rayleigh-Ritz method was used in [2] to find the frequency of the lowest mode of vibration. The relationship for the fundamental frequency for a circular plate having density ρ_d and oscillating in a medium with density ρ_m was found to be:

$$f_1 = \frac{10.21}{a^2\sqrt{1+\beta}}\sqrt{\frac{gD}{\rho_d h}} \tag{1}$$

where β and D are given by:

$$\beta = 0.6689\frac{\rho_m}{\rho_d}\frac{a}{h}, \tag{2}$$

$$D = \frac{Eh^3}{12(1-\mu^2)}. \tag{3}$$

E = Young's modulus; μ = Poisson's ratio; a = diaphragm radius; g = acceleration of gravity; h = diaphragm thickness.

The relations above were derived assuming that the deflection of the diaphragm is small compared to its thickness. In our work, this was true only for the first stage of the experiments. If the vibrating diaphragm is under considerable pressure, the stretching of the middle surface of the diaphragm also should be taken into account. In this case, the deflection produced by the pressure is comparable to the thickness of the plate. The energy of stretching is added to the energy of bending. The expression for the potential energy of bending (V) contains a term that depends on the ratio between the deflection at the center of the plate (a_1) and the diaphragm thickness (h). This potential energy has the form [3]:

$$V = \frac{32}{3}\pi D\frac{a_1^2}{a^2}\left(1+0.224\frac{a_1^2}{h^2}\right). \tag{4}$$

The oscillations of the diaphragm are not isochronic, and the frequency increases with the amplitude of oscillation. Eq. (1) gives the oscillation frequency becomes in this case:

$$f_1 = \frac{10.21}{a^2\sqrt{1+\beta}}\sqrt{\frac{gD}{\rho_d h}}\sqrt{\left(1+1.464\frac{a_1^2}{h^2}\right)}. \tag{5}$$

In reality, the diaphragm is the subject of forced oscillations. In this case, the amplitude of the forced oscillations increases by a factor proportional to the ratio between the frequency of the oscillating pressure (f) and the natural frequency (f_1) of the diaphragm. The expression of the amplitude of the forced oscillation (a_{1f}) as a function of static deflection (y_{sn}) and of the frequencies described above is derived in [3] for sinusoidal excitation with frequency f:

$$a_{1f} = y_{sn}\frac{1}{1-\frac{f_1}{f}}\sin(2\pi ft). \tag{6}$$

Resonance occurs at $f = f_1$. At this frequency the system damping assures a finite but high value for the amplitude. The additional bending stress discussed above may

Manuscript received February 7, 2002; accepted April 19, 2002. This work was supported by a grant from Waren-Rupp Inc.

The authors are with the Electrical Engineering Department, University of Akron, Akron, Ohio 44325 (e-mail: rc17@uakron.edu).

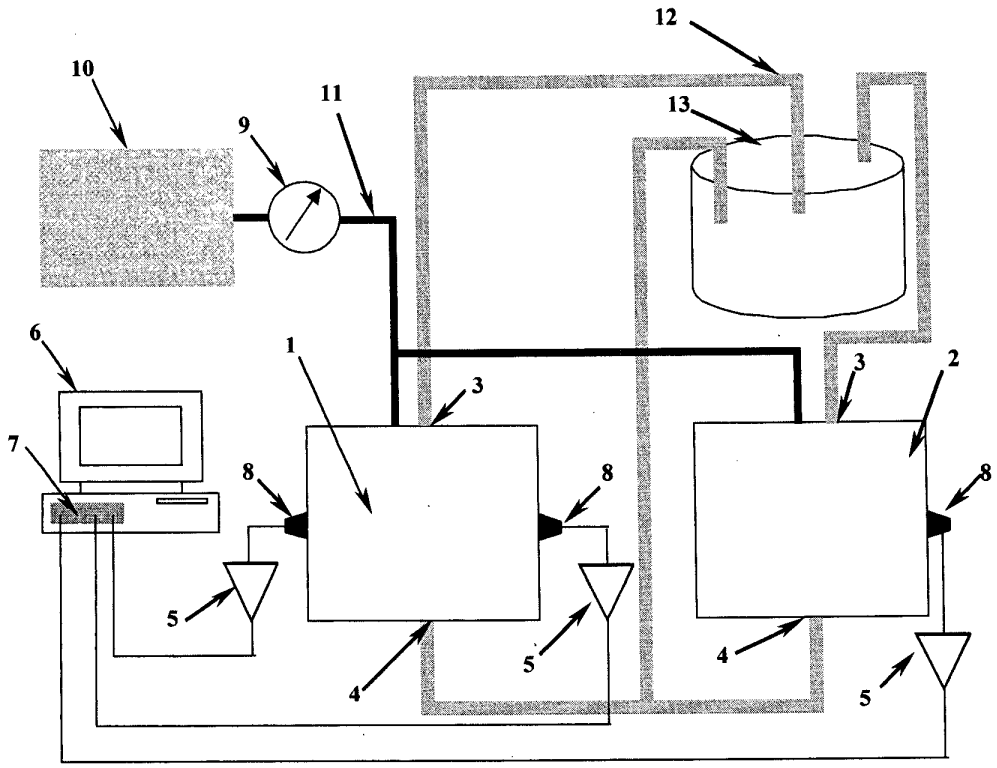

Fig. 1. Block diagram of the experimental set-up: 1, pump under test; 2, monitor pump; 3, discharge port; 4, suction ports; 5, amplifiers; 6, computer; 7, data acquisition board; 8, microphones; 9, manometer; 10, compressor; 11, air line; 12, water lines; 13, water tank.

result in initiation, and subsequent gradual development of cracks in the radial direction. Crack initiation and propagation will affect the distribution of pressure around the diaphragm and subsequently its frequency response. Eq. (6) shows that, by monitoring the frequency behavior of the diaphragm, it is possible to determine the moment when a crack is initiated. This event will be characterized by an increase [according to (5) and (6)] followed by a sharp drop in frequency. The fall in frequency is due to a decrease in the applied pressure to the diaphragm that starts when a crack is initiated.

Extensive laboratory work was necessary to identify the frequency component related to the diaphragm behavior under different operating conditions and to prove that the method is feasible. Diaphragms with different artificial flaws were mounted in the pump, and the corresponding spectra have been recorded. The spectra recorded for a flawless diaphragm (ND), for a diaphragm with a radial flaw (RD), and for an unbalanced diaphragm (UD) are shown in Fig. 2. The length of the artificial radial flaw is 1/150 of the diaphragm diameter. A 200 Hz change in the spectrum corresponding to the diaphragm with the small radial flaw, RD in Fig. 2, with respect to the spectrum of the flawless diaphragm, ND in the Fig. 2 can be seen. A larger displacement (980 Hz) appeared when the artificial flaw severely perturbed the diaphragm's operation. To model such a severe perturbance, an extra load was attached to the diaphragm. The spectrum obtained in this case, UD in Fig. 2, has a maximum at 2.29 kHz. This decrease in frequency is consistent with similar phenomena reported in the literature [4] for metallic diaphragms. The effect of additional mass m added at the center of a thin circular diaphragm (with mass M) rigidly clamped and that oscillates in a medium with longitudinal wave speed c_1 is given by [4]:

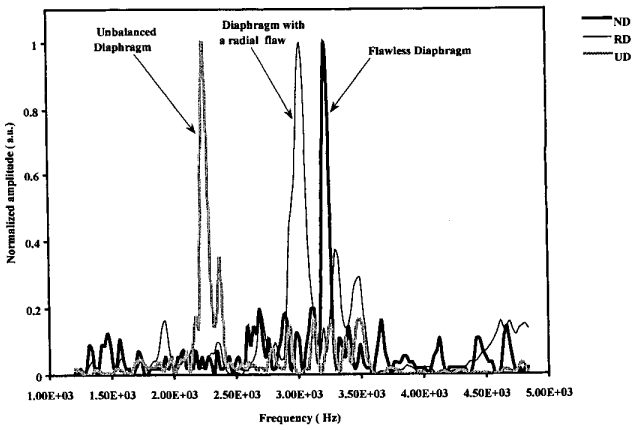

Fig. 2. Comparison between three spectra obtained for: ND, normal diaphragm; RD, a diaphragm with a small radial flaw (flaw length = 1/150 diaphragm diameter); UD, unbalanced diaphragm (a small load was attached to the diaphragm).

$$f = \frac{0.475}{\sqrt{1 + \frac{5m}{M}}} \frac{hc_1}{a^2}. \tag{7}$$

The experimental set-up used to monitor the changes in frequency response of the diaphragms is described in Section III.

III. Experimental Set-up

The block diagram of the experimental set-up used in this work is shown in Fig. 1. The acoustic signal from the pump is sensed using a miniature microphone placed outside the pump, in close proximity to or attached to the body of the pump (8 in Fig. 1). The electric signal from the microphone is amplified with a simple op-amp audio amplifier (5 in Fig. 1) before it is fed to the data acquisition board. A 16-bit data acquisition board with 200 Ks/s maximum sampling rate and 8 analog input channels was used in these experiments. For all experiments, the sampling rate was set at 25 kHz on each channel. For each channel, the input signal was sampled in a sequence of 1024 data points. This sequence represented one measurement for one channel. The digital Fourier transform of each sequence was preceded by a windowing (Hamming window) applied to the input signal. A high-pass filter also was applied to the spectra to remove the low frequency components (below 150 Hz). In addition to the data acquisition and digital processing during the acquisition process, the software package performs other tasks such as data display, data save, and spectra parameters extraction. The parameters extracted from the spectra were the frequency peak and power peak. The power peak was computed as the ratio between the spectra from a selected number (span) of lines around the peak frequency and equivalent noise bandwidth of the selected window (ENBW), using the following [5]:

$$\mathrm{PP} = \frac{\sum_{j} \text{Power Spectrum}(j)}{\mathrm{ENBW}} \quad \text{for } \mathrm{j} = 1 - \mathrm{span}/2, \ldots, \mathrm{i} + \mathrm{span}/2, \quad (8)$$

where i is the index of the frequency peak. To increase the speed of data processing, C-compiled subroutines were used.

Measurements were performed at intervals of 10 seconds. A complete data structure was saved as a single record to guarantee sequential access to the data. The data structure used consists of the following: data, clock time, frequency peak for channel 1 (CH1), power peak for CH1, frequency peak for CH2, power peak for CH2, frequency peak for CH3, power peak for CH3. After each 180 measurements (one-half hour), the full waveforms acquired from each channel also were included in the recorded data for possible future evaluation and display. Sequential access to the data was an important issue because the number of measurements recorded in the experiments was very large (between 17700 and 118715).

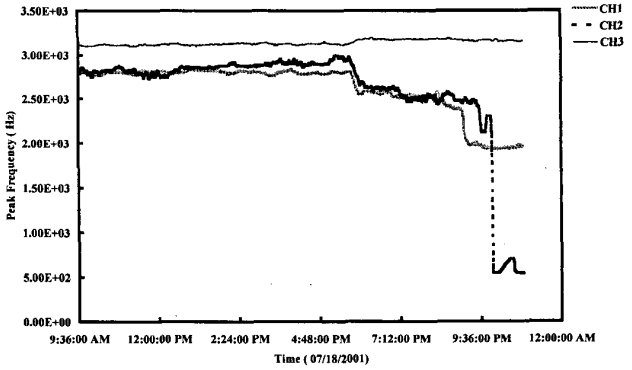

Fig. 3. Data recorded in experiment 2 demonstrates that a "failure initiation event" appeared only at pump 1 on channel 2 (CH2, dashed line) at 6:15 PM. This event is characterized by a sharp drop, preceded by a small increase in frequency.

IV. Experimental Results

The results obtained in laboratory experiments helped to set the parameters for in-plant measurements. In these experiments, the background noise was much higher than in the laboratory; and additional pumps were operating in very close proximity to the pump under test. In these tests, the air pressure was set at or near the limit of the pump's specifications to encourage failure. The time when bubbles first appear in the water tank (13 in Fig. 1) was recorded by an operator as the pump's time of failure. The data recorded shows that the automated system responded promptly to the pressure variations in the pump (shutdowns). For a 1-minute shutdown, a variation of 90% in the power peak between measurements recorded in two successive measurements (10 seconds apart) was observed.

Fig. 3 shows the failure initiation event as recorded by the system. A median filter over 50 recorded points was used for these representations. Fig. 3 shows a major change in the behavior of pump 1 (CH1 and CH2) on July 18 at 6 PM. At this instant, a "failure initiation event" appeared at 6 PM on CH2 (in Fig. 3). This event is characterized by a sharp decrease in frequency preceded by a 100 Hz increase. A decrease is noticed on CH1 as well because of acoustic coupling between the two channels, but the subsequent evolution of the signal is different. The peak frequency on CH2 continues its fall until it reaches a value of 500 Hz. However, the frequency on CHl 1 has stabilized for the remainder of the experiment at 2 kHz. No change is observed on monitor CH3. A difference between the behavior of CH1 and CH2 is noticed at 9 PM in Fig. 3. At this instant, a larger change in CH2 (dashed curve in Fig. 3) than that in CH1 is visible. Note from Fig. 3 that CH1 continues to operate normally. The diaphragm monitored by CH2 failed at 10 PM as confirmed by operator observations. The most important aspect of this method is that there is a significant time between failure initiation and actual failure. In the case shown here, there are approximately 4 hours during which action may be taken before rupture of the diaphragm occurs.

The third experiment was performed for 14 continuous days (partly to test the capability of the system to manage large amounts of data) with three separate failures, all confirming the results above. The experiment consisted of three different tests. In these tests, each channel played, in turn, the role of the monitor channel.

V. Conclusions

This work proposes a new method for the detection of failure initiation in elastic diaphragms of air-driven pumps. The method is based on frequency analysis of the acoustic signal emitted by the pump during its normal operation. Laboratory tests have shown that the presence of different artificial flaws can be detected. Three in-plant experiments have shown that a failure initiation event can be detected from frequency behavior analysis for each test, and that a subsequent failure occurs. The time between failure initiation and actual failure is significant and may be used to take corrective action.

Acknowledgments

The assistance of Mr. Ricardo Matias and Mr. Eric Rinaldo in performing the laboratory data is greatly appreciated. The authors would like to thank Mr. David Roseberry for his help in obtaining the in-plant experimental data.

References

[1] P. M. Morse and K. U. Ingard, *Theoretical Acoustics*. New York: McGraw-Hill, 1968, pp. 209–222.

[2] C. M. Harrys, *Shock and Vibration Handbook*. New York: McGraw-Hill, 1996, pp. 7.38–7.45.

[3] S. Timoshenko, *Vibration Problems in Engineering, 3rd ed.* Princeton, NJ: Van Nonstrand, 1955, pp. 449–455.

[4] J. H. Powell and J. H. T. Roberts, "On the frequency of vibration of circular diaphragms," in *Proc. Physical Soc. London*, Apr. 1923, pp. 170–182.

[5] *LabView Analysis VI: Reference Manual*. Austin, TX: National Instruments Corp., 1996, pp. 4.4–4.12.